Full-waveform inversion using the one-way wave equation

Claudio Guerra and Carlos Cunha, Petrobras

Abstract

The classical full-waveform inversion is a method for obtaining detailed velocity models of the subsurface, formulated as an inverse problem, in which modeling and adjoint operators use the two-way wave equation. Solving the wave equation with the two-way propagator is computationally demanding when compared to the less accurate one-way propagator. However, the range of validity of the one-way wave equation is quite reasonable for most of the geological environments in which exploration has been carried out. For these situations, we propose to perform full-waveform inversion based on the first-order Born approximation, using the one-way propagator which promises to be less computationally intensive than the classical FWI. Our approach includes defining the objective function by cross-correlation to mitigate the impacts that cycle-skipping and amplitude differences have on the solution, and improving the gradient information by deconvolving and integrating the back-propagated residuals to accelerate convergence.

Introduction

In the last years, research on velocity model definition has shifted from ray to wave methods. More recently, increasing interest has been put on full-waveform inversion (FWI), especially after the impressive 3D real data results obtained by Sirgue et al. (2009). Nevertheless, fundamental issues like data incompleteness and initial velocity-model accuracy, which impact the convergence speed, are still open questions. To address them, different strategies (Boonyasiriwat et al., 2009) and objective functions (Luo and Schuster, 1991) have been proposed.

Classical FWI in 3D is becoming feasible pushed by more efficient two-way propagators as well as decreasing cost of computer clusters. Despite these factors, FWI is still an expensive process and its routine use is far from being a reality. For some geological scenarios, where steep propagation angles in laterally varying media and turning waves are not carriers of significant information, using the cheaper one-way propagators (OWP) produces accurate, high quality images. In these cases, one-way propagators can be used to perform FWI. Alternatively, if steep propagation angles carry important information, OWP with meshes conforming to the direction of turning-wave propagation can be used (Shragge, 2007).

Our inversion scheme uses the cross-correlation objective function, similar to the wave-equation traveltime inversion of Luo and Schuster (1991). This objective function is less sensitive to cycle-skipping and amplitude differences between observed and one-way modeled data. Two different cross-correlation objective functions are used: a trace/trace correlation and a trace/trace correlation in a running window. An important advantage of this approach is that it allows us to simultaneously invert for all the wavenumbers present in data without the need of a multi-scaling strategy.

It is desirable that the gradient of the objective function has a layered structure, mimicking velocity distribution, to accelerate convergence. Ma et al. (2010) showed that using an image-guided gradient allows fast convergence to an adequate velocity model. Instead of using structural properties of the gradient, here we compute the pseudo-impedance correspondence of the gradient. For that, we deconvolve the wavelet present in the back-propagated residuals. The deconvolution assumes that illumination is perfect. Ideally, lest-squares migration should be used for this task. The deconvolved back-propagated residuals are subsequently integrated to generate a blocky representation of the gradient.

Next, we review FWI and describe our methodology. In the examples, we show the validity of our approach using simple synthetic data and field data from the Santos Basin.

Method

The theoretical background of FWI can be found in Tarantola (1984). FWI is an optimization problem in which waveform differences between the observed data (d_0) and the modeled data (d) are minimized. In out approach, data d are computed using Born modeling, which, in the frequency domain, reads

$$d\left(\mathbf{x_s},\mathbf{x_r};\omega\right)=\omega^2\int G_s(\mathbf{x_s},\mathbf{x};\omega)r(\mathbf{x})G_r(\mathbf{x},\mathbf{x_r};\omega)d\mathbf{x}, \quad (1)$$

where ω is the radial frequency, $\mathbf{x_s}$, $\mathbf{x_r}$, and $\mathbf{x}$ are shot, receiver, and model position vectors, respectively. In the present case, G_s is the source one-way Green´s function and G_r is the receiver one-way Green´s function computed using the velocity of the current FWI iteration. The reflectivity r is obtained by deconvolving the wavelet (explained in the sequence) in the image of the current iteration.

Here, we aim at minimizing, in the l_2 sense, the traveltime differences between the observed and the modeled data, following the lines of Luo and Schuster (1991). The traveltime differences are determined by measuring the lag $\Delta\tau$ of the maximum cross-correlation ϕ

$$\phi(\mathbf{x}_\mathrm{S}, \mathbf{x}_\mathrm{r}, \tau) = \int d_0(\mathbf{x}_\mathrm{S}, \mathbf{x}_\mathrm{r}, t+\tau) d(\mathbf{x}_\mathrm{S}, \mathbf{x}_\mathrm{r}, t) dt. \quad (2)$$

The mathematical representation of the problem does not change; irrespective we use the windowed trace/trace correlation.

The objective function $J(v)$ is

$$J(v) = \frac{1}{2} \|\Delta\tau(\mathbf{x}_\mathrm{S}, \mathbf{x}_\mathrm{r})\|^2. \quad (3)$$

For the velocity update, we need to compute the gradient of (3) with respect to the velocity, using

$$\nabla J(\mathbf{x}) = \frac{\partial \Delta\tau}{\partial v} \Delta\tau, \quad (4)$$

which, after some algebra, reads for one frequency

$$\nabla J(\mathbf{x}; \omega) = \int\int G_s^*(\mathbf{x}_\mathrm{S}, \mathbf{x}; \omega) G_r^*(\mathbf{x}, \mathbf{x}_\mathrm{r}; \omega) \hat{d}_0(\mathbf{x}_\mathrm{S}, \mathbf{x}_\mathrm{r}; \omega) d\mathbf{x}_\mathrm{S} d\mathbf{x}_\mathrm{r}, \quad (5)$$

where $\hat{d}_0(\mathbf{x}_\mathrm{S}, \mathbf{x}_\mathrm{r}; \omega) = d_0(\mathbf{x}_\mathrm{S}, \mathbf{x}_\mathrm{r}, t) \Delta\tau(\mathbf{x}_\mathrm{S}, \mathbf{x}_\mathrm{r}, t)$ and the asterisk represents complex conjugate. The final gradient is obtained after summing over all the frequencies. Notice that the gradient corresponds to the migration of the observed data weighted by the lag of the maximum cross-correlation. If this lag is zero, observed data and modeled data perfectly match, so the gradient is zero and no velocity update is required.

As the back-projected residuals strongly resembles reflectivity since it is basically migration of the observed data after weighting, we transform the reflectivity-like information of the back-projected residuals into a pseudo-impedance-like one by deconvolving the remaining wavelet and integrating (Rosa, 2010) to accelerate convergence. The reasoning is that velocity is more related to impedance than to band-limited reflectivity. This procedure can also be applied when FWI is performed with the two-way wave equation. Ma et al. (2010) compute a blocky gradient based on its structural information. They achieve faster convergence with this blocky gradient than that obtained with the conventional gradient.

Deconvolving and integrating the back-projected residuals generates important low-wavenumber information that, in general, is absent in the observed data. This procedure assumes complete illumination of the reflectors. When this is not the case, a least-squares migration scheme should be applied prior to integration. For now, we are not considering the effect of density on impedance. The pseudo-impedance-like transformation is illustrated in 1D in Figure 1. The original impedance model is represented by three layers of constant impedance. The input seismic trace (trace 1) is computed by convolving a Ricker wavelet with the reflectivity model derived from the impedance model. After deconvolution (trace 2) it is integrated (trace 3) recovering the impedance information. Trace 4 shows the result of applying integration without deconvolving trace 1.

In 2D or 3D, especially when applying on real data, trace-to-trace differences introduce strong lateral variations of the low-vertical-wavenumber component of the pseudo-impedance-like gradient. These lateral variations are corrected by applying trapezoidal filters that act as bandpass filters. This issue will be illustrated in the Results section.

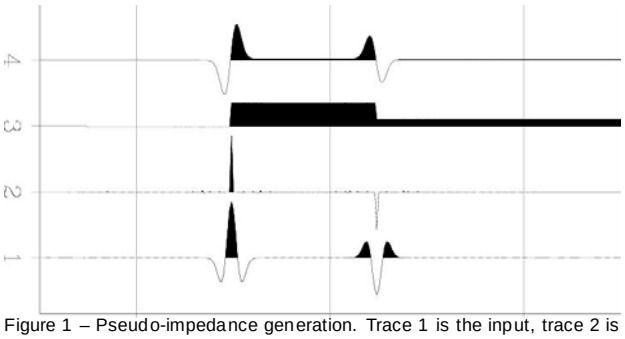

Figure 1 – Pseudo-impedance generation. Trace 1 is the input, trace 2 is the deconvolution of trace 1, trace 3 is the integration of trace 2 emulating the impedance, and trace 4 is the integration of trace 1.

Examples

To illustrate the one-way FWI strategy, we use the sediment portion of the Sigsbee2a model (Paffenholz et al., 2002). We use Born modeling to synthesize 67 shots with 300 ft shot spacing, maximum offset 45,000 ft, and frequency range of 4-60 Hz. The reflectivity model was obtained from the original velocity (Figure 2a). By doing so, data and modeling/migration algorithms used the inversion scheme are consistent.

The initial velocity model is the migration velocity of Sigsbee2a, which is basically a 1D velocity function hung at the water bottom (Figure 2b). Initially, we used the trace/trace correlation objective function in the inversion. Data residuals were median-smoothed along the time, offset, and shoot axes. The gradient was median-smoothed as well. The corresponding final velocity model (Figure 3) converged after 4 iterations and highly resembles the original velocity.

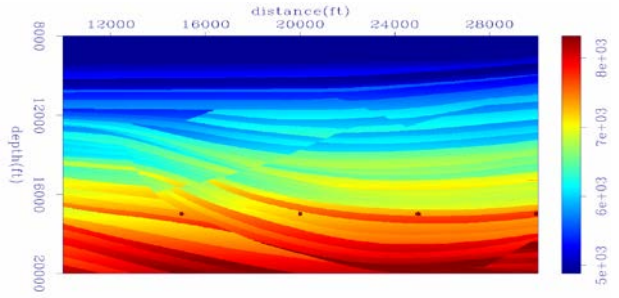

(a)

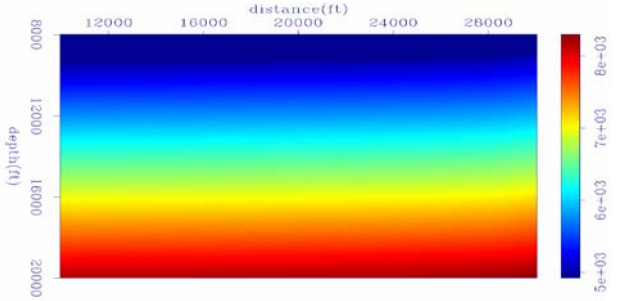

(b)

Figure 2– The original velocity model used to model data (a) and the initial velocity model input to FWI (b).

Then, this inverted velocity model is used as input for a new run of inversion, but now using the windowed trace/trace correlation. By doing this, we expect to invert for finer details of the velocity model. In fact, the objective function decreased 4.75% and only one iteration was accepted, not adding much of the expected details to the velocity model.

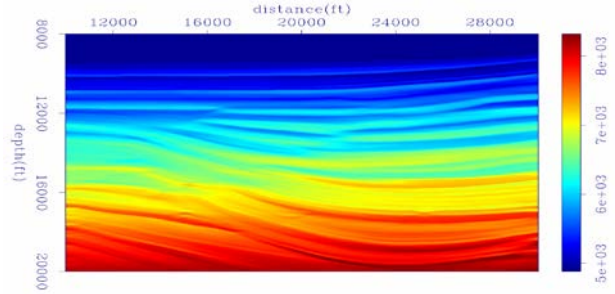

Figure 3– The velocity model inverted with trace/trace correlation objective function input to a new run of FWI with windowed trace/trace correlation objective function.

Results

We applied the methodology on the shallow portion of a marine dataset from the Santos Basin, Brazil. We selected the nearest cable to source, the maximum offset is 8225 m, and the frequency range is 4-40 Hz. The initial velocity model (Figure 4a) is taken from a 3D interval velocity cube for PSDM. After 12 non-linear iterations, inversion stopped without decreasing the objective function and we obtained the optimized velocity model of Figure 4b.

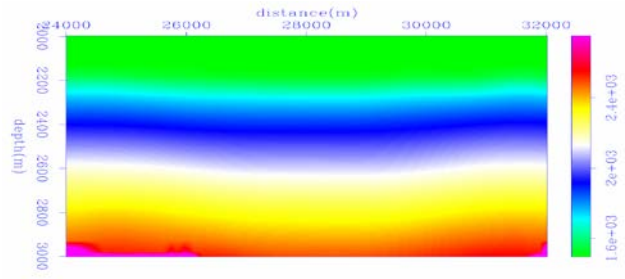

(a)

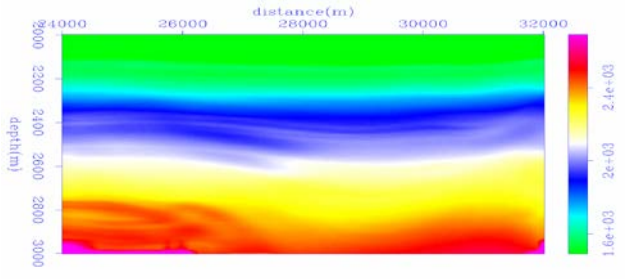

(b)

Figure 4– The initial velocity model derived for PSDM (a) and the final velocity model after FWI (b).

The deconvolution of the residual wavelet is a 1D process with no constraint on the spatial variation of the wavelet. For the back-projected residuals, the spatial variation of the wavelet is caused not only by variations of the source from shot-to-shot (here we use only one source function), but also by high-frequency variations of the crosscorrelation lags. The variation of the correlation lags can be mitigated by using a strong smoothing at the expense of lack of resolution of the objective function. Otherwise, when submitting the back-propagated residuals (Figure 5a) to the pseudo-impedance transformation by integration, an inaccurate DC-component occurs with high-spatial variation after integration (Figure 5b). This inaccuracy in the DC component is suppressed by applying trapezoidal filters, which act as bandpass filters (Figure 5c).

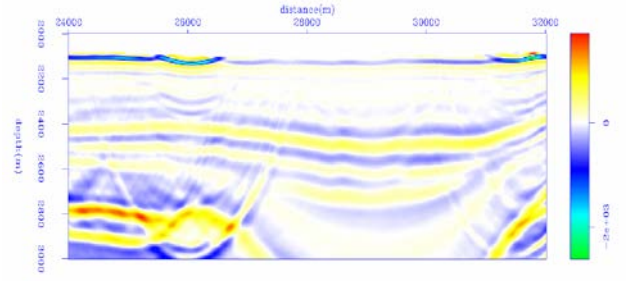

(a)

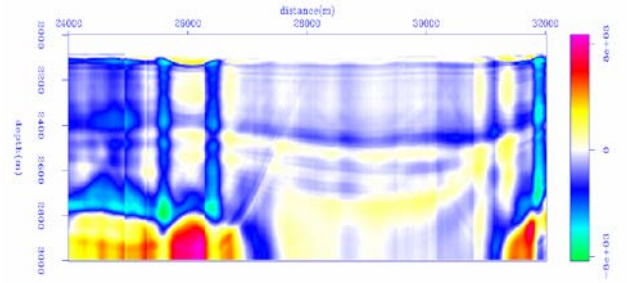

(b)

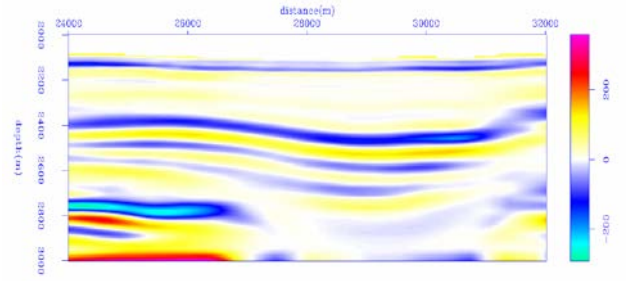

(c)

Figure 5 – Computation of the pseudo-impedance-like back-propagated residuals: a) back-propagated residuals; b) integration of (a); and c) trapezoidal filtering of (b).

The evolution of the objective function is presented in Figure 6.

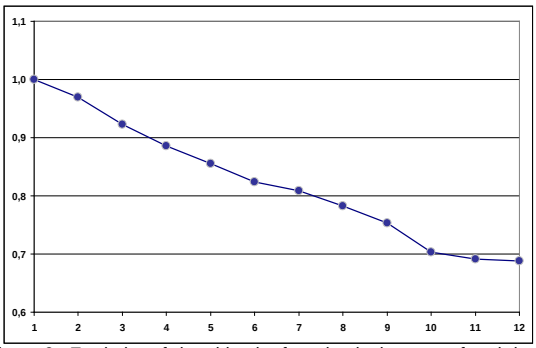

Figure 6– Evolution of the objective function in the case of real data.

For the Born modeling we need an intermediate migrated image with the current velocity. Similar to the stack-power objective function of Chavent and Jacewitz (1995), we compute the RMS amplitude of this image as a measure of focusing. For now, we are not using this measure as a metric in the inverse problem. Figure 7 shows that this RMS amplitude overall increases about 10%, indicating that velocity updates produce a better focused image throughout the iterations. This is can be an indication that this objective function could be used in conjunction to the crosscorrelation objective function in the future.

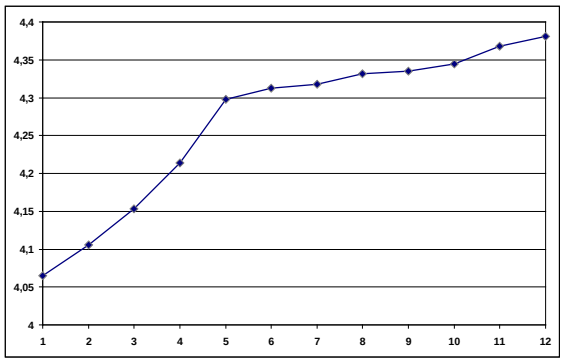

Figure 7 – RMS amplitude of the migrated images per iteration.

Migration with the velocity models of Figure 4 produced the images of Figure 8. The stacked section (Figure 8a) does not change significantly, whether we migrate with the original velocity (Figure 4a) or with the optimized velocity (Figure 4b). Angle gathers were computed from -40° – 0°. Figures 6b and 6c show angle gathers from spatial coordinate 27,000 and 30,000, and from depth 2,300 m to 3,000 m. The ones resulting from migration with the optimized velocity (Figure 8c) are a bit flatter than that computed with the original velocity (Figure 8b). Of course, 3D effects like cable feathering and out of plane events must have some impact on the results.

Conclusions

We showed that under relatively simple geology one-way propagator can be used to perform FWI at a low computational cost. Compared to the classical FWI, the cost is decreased by using a cheaper propagator and by accelerating convergence using the pseudo-impedance-like gradient. One interesting feature of the strategy is that the cross-correlation objective function allows for simultaneously inverting of the full bandwidth. For now, it is extremely important to have an adequate phase treatment of the input data, which must be zero-phase. Relaxing this restriction is part of future work. To determine the range of validity of our strategy demands more testing in geologically complex environments.

Acknowledgments

We would like to thank Petrobras for allowing the publication of this paper.

References

Boonyasiriwat, C., P. Valasek, P. Routh, W. Cao, and G. T. Schuster, 2009, An efficient multiscale method for time-domain waveform tomography: Geophysics, 74, no. 6, WCC59–WCC68.

Chavent, G. and Jacewitz, C.A., 1995, Determination of background velocities by multiple migration fitting: Geophysics, 60, no. 2, 476-490.

Ma, Y., Hale, D., Meng, Z., and Gong, B., 2010, Full waveform inversion with image-guided gradient: SEG Technical Program Expanded Abstracts, 1003-1007.

Paffenholz, J., McLain, B., Zaske, J., and Keliher, P.J., 2002, Subsalt multiple attenuation and imaging: Observations from the Sigsbee2B synthetic dataset: SEG Technical Program Expanded Abstracts, 2122-2125.

Rosa, 2010, Análise do sinal sísmico: Sociedade Brasileira de Geofísica (SBGf), 668pp.

Shragge, J., 2007, Waveform inversion by one-way wavefield extrapolation: Geophysics, 72, no. 4, A47-A50.

Sirgue, L., Barkved, O. I., Van Gestel, J. P., Askim, O. J., and Kommedal, J. H., 2009, 3D waveform inversion on Valhall wide-azimuth OBC: EAGE expanded abstracts, U038.

Tarantola, A., 1984, Inversion of seismic reflection data in the acoustic approximation: Geophysics, 49, no.8, 1259-1266.

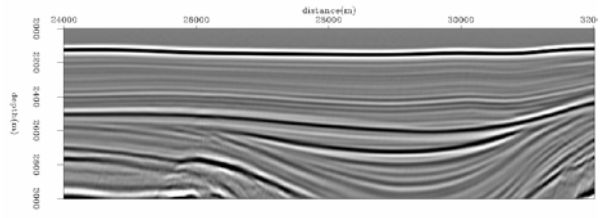

(a)

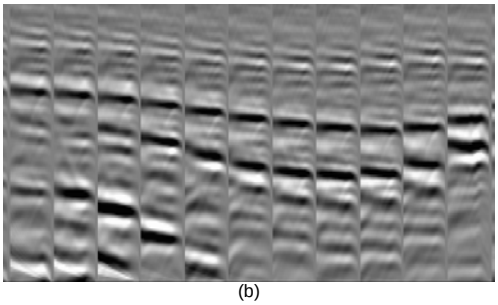

(b)

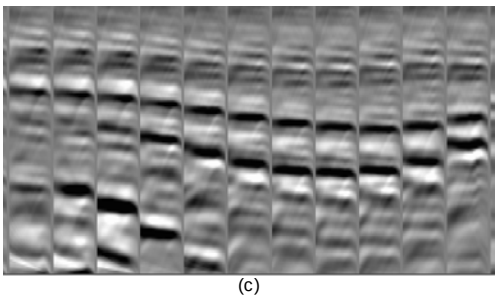

(c)

Figure 8 – Real data example: a) Image migrated with the original velocity for PSDM, b) Angle gathers computed with the original velocity, and c) Angle gathers computed with the optimized velocity. Reflection angles increase from right to left within the gathers.